ELSEVIER

Available online at www.sciencedirect.com
SCIENCE DIRECT®

Polymer 45 (2004) 197–206

polymer

www.elsevier.com/locate/polymer

Reactively formed block and graft copolymers as compatibilizers for polyamide 66/PS blends

Hyun K. Jeon[a,*], Benjamin J. Feist[a,1], Sok Boon Koh[a,2], Kwanho Chang[a],
Christopher W. Macosko[a], Robert P. Dion[b]

[a]*Department of Chemical Engineering and Materials Science, University of Minnesota, Minneapolis, MN 55455, USA*
[b]*Corporate Research and Development, Dow Europe GmbH, Bachtobelstrasse 3, CH-8810 Horgen, Switzerland*

Received 29 August 2003; received in revised form 24 October 2003; accepted 28 October 2003

Abstract

Phthalic anhydride terminated polystyrene (PS-An) and styrene-maleic anhydride copolymer (SMA) were compared as a compatibilizer at low loadings (<10 wt%) in 70/30 polyamide 66 (PA66)/polystyrene (PS) blends. Compatibilization efficiency was judged by morphology of the blends and the extent of interfacial coupling to copolymer. Fluorescent labels of functional PS's (anthracene and pyrene for PS-An and SMA, respectively) allowed the detection of small amounts of reactively formed block (PA66-*b*-PS) or graft copolymer (SMA-*g*-PA66) in the blends via gel permeation chromatography with a fluorescence detector. Extremely fast reactions giving $>60\%$ conversion in 0.5 min mixing were observed regardless of the molecular weight, the structure, and the amount of the functional PS's. Interfacial stability of the reactively formed copolymers was estimated by micelle formation in the bulk phases and the interfacial coverage, Σ. PS-An with higher molecular weight (37 kg/mol) was most effective as a compatibilizer at the interface, showing less tendency to form microemulsions by suppressing interfacial roughening. However, a large portion of PA66-*b*-PS from low molecular weight PS-An (10 kg/mol) and SMA-*g*-PA66 from random functional SMA (16 kg/mol) migrated to the bulk phase to form micelles even at <2 wt% loadings. Blends of PA66 with syndiotactic PS compatibilized with PS-An gave very similar morphology to the PA66/PS blends indicating that these conclusions apply also to PA66/sPS blends.

Keywords: Reactive compatibilization; Interfacial stability; Molecular architecture

---

1. Introduction

Polyamides (PA) are engineering plastics with various commercial applications due to their outstanding properties [1]. In order to meet specific applications, PA have also been blended with commercial polyolefins containing functional groups which react with amine and/or carboxylic acid end groups of PA [1,2]. PA/polystyrene (PS) blends have also been of interest since incorporation of various functional groups such as maleic anhydride [3,4], glycidyl methacrylate [5], and acrylic acid [6] to PS is relatively easy. As well, functionalized PS's have been used as compatibilizers for PA/poly(2,6-dimethyl-1,4-phenylene oxide) (PPO) blends because of its miscibility with PPO [7,8].

Recently, syndiotactic PS (sPS) has attracted attention for blends with PA due to its excellent resistance to heat and chemicals originating from its crystallinity [9–12] It is reasonable to consider functional amorphous PS's as compatibilizers for the incompatible PA/sPS blends since they are miscible with sPS [13]. However, it should be noted that the amount of functional PS in the blends should be kept as low as possible not to deteriorate the desirable properties. Therefore, it is necessary to find an appropriate functional PS satisfying the demand to be used in PA/sPS blends. To judge the efficiency of a reactive compatibilizer, the reactivity of complimentary functional polymers at the interface should be considered, since the amount of reactively formed copolymer formed at the interface controls dispersed particle size and interfacial adhesion.

---

[*] Corresponding author. Tel.: +1-612-625-0584; fax: +1-612-626-1686.
E-mail address: jeon@cems.umn.edu (H.K. Jeon).

[1] Present address: Department of Chemical Engineering, University of Delaware, Newark, DE 19716, USA.

[2] Present address: Department of Materials Science and Engineering, University of California Los Angeles (UCLA), Los Angeles, CA 90095-1595, USA.

0032-3861/$ - see front matter © 2003 Elsevier Ltd. All rights reserved.
doi:10.1016/j.polymer.2003.10.099

Another important criterion is the stability of a reactively formed copolymer at the interface. It has been suggested that molecular weight and structure of functional polymers play important roles on the interfacial stability as well as the reactivity of functional groups [14–21].

In this study, we aimed at investigating the effect of molecular structure of reactively formed copolymers on compatibilization for polyamide 66 (PA66)/PS, a model system for PA/sPS blends. Various low concentrations of functional PS's were added to the blends. Morphology of the blends and conversion to copolymer by interfacial coupling were the criteria for determining the efficiencies of compatibilizers. Two phthalic anhydride terminal PS's (PS-An) with different molecular weights were used to study the effect of molecular weight on compatibilization efficiency. The difference between reactively formed block and graft copolymers in compatibilization was explored by comparing blends with styrene-maleic anhydride random copolymer (SMA) to the PS-An results.

2. Experimental

2.1. Materials and characterization

Characteristics of polymers used in this study are summarized in Table 1. PA66 was from Solutia, Inc. (Vydyne21^{TM}). PS and sPS were obtained from the Dow Chemical Company (Styron685^{TM} and Questra^{TM}, respectively). PS18 was synthesized by anionic polymerization. Number average molecular weight (M_n) and weight average molecular weight (M_w) of amorphous PS's were determined by GPC based on PS standard samples. Absolute number average molecular weight (M_n) of PA66 was measured by titration of end groups. The acid end groups were titrated in benzyl alcohol with tetrabutyl ammonium hydroxide, and the amine end groups were titrated in hexafluoroisopropanol with hydrochloric acid (HCl). Complex viscosities, η^*, of polymers were measured at 270 and/or 280 °C with a rheometer (ARESII, Rheometric Scientific Inc.). Table 1 shows η^* at 100 rad/s which was the maximum shear rate in the mixer during blending.

Table 1
Characteristics of polymers used

Polymer	M_n (kg/mol)	M_w/M_n	Functionality (f)	Fluorescent group	η^* (Pa s) at 100 rad/s
PA66	15.5	2.1[a]	0.35 NH_2	–	576[b] 489[c]
PS	160	2.03	–	–	422[b]
sPS	250		–	–	481[c]
PS18	18	1.05	–	–	–
PS-An-10	10	1.2	0.85	Anthracene	–
PS-An-40	37	1.2	0.75	Anthracene	–
SMA	16	1.5	6.4	Pyrene	–

[a] M_w/M_n was determined using GPC with PS standards after trifluoroacetylation.

[b] Viscosity measured at 270 °C.

[c] Viscosity measured at 280 °C.

2.1.1. Trifluoroacetylation of PA66

In order to use GPC, PA66 was modified via trifluoroacetylation as shown in Fig. 1 [22,23]. 50 mg of PA66 was added to a flask capped with a rubber septum, and the flask was flushed with Ar or N_2 through a hypodermic needle for 10 min. 1.5 ml dry methylene chloride (CH_2Cl_2) was added to the flask followed by the addition of a three-fold molar excess of trifluoroacetic anhydride (TFAA). The reaction was allowed to run until PA66 pellets dissolved completely at 25 °C. Then, TFAA modified PA66 (TFAA-PA66) was isolated by evaporating CH_2Cl_2, excess TFAA, and trifluoroacetic acid (TFA). 1 ml dry CH_2Cl_2 was added again to dissolve TFAA-PA66. Adding CH_2Cl_2 helped to dissolve TFAA-PA66 in dry THF to prepare GPC samples with a concentration of 1 mg/ml. The GPC sample had to be run within a few hours after sample preparation, otherwise polymer crystallized from the GPC solution after about a day. Fig. 2 shows the GPC trace of PA66 from a refractive index (RI) detector. The relative M_n and M_w/M_n were measured to be 33.5 kg/mol and 2.1, respectively, based on PS standards.

2.1.2. End-functional PS (PS-An)

Phthalic anhydride end-functional PS labeled with anthracene (PS-An) was synthesized by atom transfer radical polymerization (ATRP) using di-*t*-butyl phthalate (DTBP) initiator [24]. 9-Anthracenyl methyl methacrylate (anth-MMA) [25] and styrene monomers were copolymerized at 110 °C for 12 h for each chain to have 1 or 2 anthracene groups. After polymerization followed by purification, pyrolysis was carried out at 190 °C under vacuum for 1 h to close the DTBP group to phthalic anhydride. Detailed synthesis and purification procedures can be found in Refs [24,25]. Functionality of PS-An was determined by a coupling reaction with two molar equivalent of amine terminal PS ($PS-NH_2$) in dry THF for 2 days at room temperature followed by the GPC analysis with the fluorescence detector. $PS-NH_2$ was gratefully

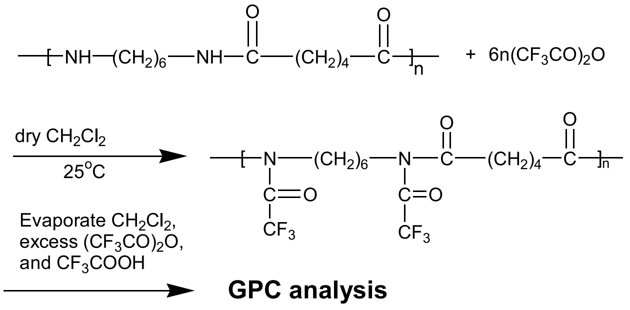

Fig. 1. Modification of PA66 via trifluoroacetylation to render it soluble in THF for GPC analysis [22,23].

supplied by Prof. Jérôme at University of Liège, Belgium. Synthesis and determination of functionality of PS-NH_2 are described elsewhere [26,27]. For PS-An with $M_n = 10$ kg/mol (PS-An-10), PS-NH_2 with $M_n = 26$ kg/mol (PDI = 1.14, $f = 0.85$) was used. Longer PS-NH_2 ($M_n = 72$ kg/mol, PDI = 1.25, $f = 0.80$) was reacted with PS-An with $M_n = 37$ kg/mol (PS-An-40).

2.1.3. Pyrene labeled maleic anhydride random functional PS (SMA)

Conventional nitroxide mediated polymerization (NMP) was carried out to synthesize styrene-maleic anhydride copolymer (SMA) using benzoyl peroxide (BPO) and 2,2,6,6-tetramethyl-1-piperidinyloxy (TEMPO) at 110 °C (see Fig. 3) [28]. Functionality and molecular weight were targeted at 11 and 25 kg/mol, respectively. 1-Pyrenemethylamine was prepared from 1-pyrenemethylamine hydrochloride (Aldrich) using hexane and ammonium hydroxide [29]. To measure functionality by ^{1}H NMR spectroscopy (Varian VI-500), SMA and 1-pyrenemethylamine (two molar equivalent based on the target functionality) were reacted in dry toluene at 100 °C for 2 days. Excess 1-pyrenemethylamine was removed by precipitating SMA into methanol. Peak intensity ratio of pyrene group (9H, $\delta = 7.6$–8.2 ppm) to phenyl group (2H, $\delta = 6.2$–6.9 ppm) was measured, and the functionality of SMA was determined to be 9 that corresponds to 5.5 wt% MA.

SMA was partially labeled with pyrene group through the same reaction route as shown in Fig. 3. It was aimed to incorporate three pyrene groups per chain. We found by ^{1}H NMR that 2.6 MA groups per SMA chain reacted with 1-pyrenemethylamine resulting in the functionality of 6.4 corresponding to 3.9 wt% MA and 5.1 wt% 1-pyrenemethylsuccinimide.

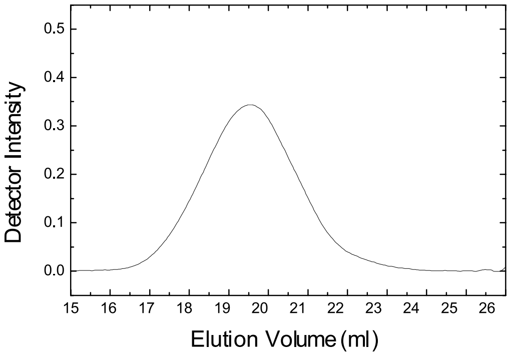

Fig. 2. GPC trace of PA66 from a refractive index (RI) detector after trifluoroacetylation.

2.2. Blend preparation and characterization

PA66/PS and PA66/sPS blends were prepared using a preheated cup-rotor mixer (Minimax CS-183MMX, Custom Scientific Instrument, Inc.) with three steel balls at 270 and 280 °C, respectively [30]. The composition of the blends with the reactive polymers was 70 wt% PA66/[20 wt% PS or sPS + $(10 - x)$ wt% PS18 + x wt% compatibilizer] with x varied from 0 to 10. PS18 was incorporated to keep the viscosity of the PS phase approximately constant with the addition of the low molecular weight functional polymers. Complex viscosity, η^*, of the PS phase consisted of 70/30 wt/wt PS/PS18 was measured to be 195 Pa s at 270 °C and 100 rad/s, and the viscosity ratio, η_r of the PS phase to PA66 was 0.34. In the case of 70/30 sPS/PS18 mixture, η^* and η_r were 126 Pa s and 0.26 at 280 °C and 100 rad/s. All the blends in this study were prepared by one-step mixing in which all the polymers were dry-blended at ambient temperature and fed to the mixer. Blend samples (~10 mg) were taken from the edge of the rotor bottom at 0.5, 2, 6, 10 and 20 min followed by quenching in liquid N_2. Reaction conversion with mixing time was measured by GPC with the fluorescence detector for PA66/PS blends. PA66 in the blends was modified via trifluoroacetylation.

Morphology of the blend samples taken at 20 min mixing was observed using scanning electron microscopy (SEM, JEOL 6500). Specimens were microtomed at −70 °C using a glass knife or cryo-fractured. PS minor phase was extracted with THF to enhance the contrast between two phases. The area of each particle was measured using image analysis software (Image Tool, UTHSCSA), and then corresponding diameter was calculated by Eq. (1). The volume to surface area average particle diameter, D_{VS}, was measured. Particles with $D_i < 0.1$ μm were not counted in the D_{VS} calculation.

$$D_i = 2\left(\frac{A_i}{\pi}\right)^{1/2} \tag{1}$$

$$D_{VS} = \frac{\sum_i D_i^3}{\sum_i D_i^2} \tag{2}$$

Transmission electron microscopy (TEM, JEOL 1210) was employed to see micelles in the blends. The blend at 20 min mixing time was cryo-microtomed at −70 °C to thin films of 50 nm. The sliced sections were exposed to RuO_4 (0.5% aqueous solution) vapor for 20 min to stain PS phase in the blends.

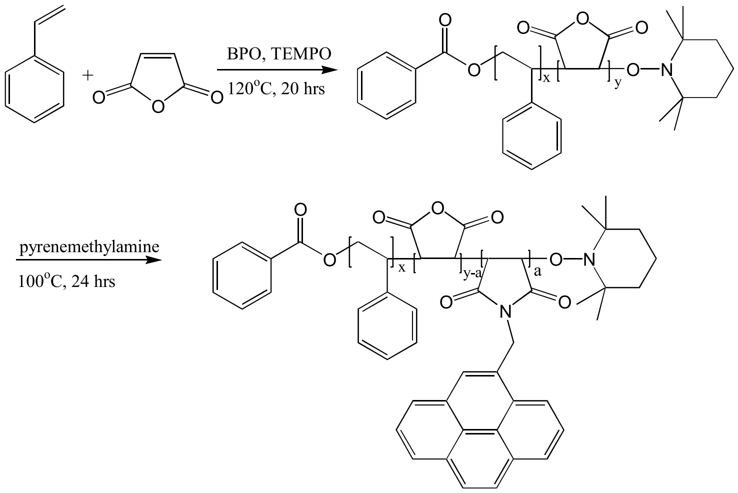

Fig. 3. Synthesis of SMA by nitroxide mediated polymerization (NMP) [28] and incorporation of pyrene group in SMA.

3. Results

3.1. Morphology

Fig. 4(a)–(c) shows the dramatic morphology change upon addition of 2 wt% PS-An to the PA66/PS blends. The blend with no compatibilizer shows a very broad distribution of particle size from ~20 to ~1 μm. In the blends with 2 wt% PS-An the particle size reduces sharply and becomes uniform (Fig. 4(b) and (c)). It can be seen that the blend with PS-An-40 has more uniform size distribution. Fig. 4(d) shows the morphology of the 1.75 wt% SMA blend. It is observed that particle size for the blend with 1.75 wt% SMA is larger than that for the blend with 2 wt% PS-An. Fig. 4(e) and (f) shows the morphology of PA66/sPS blend with no functional PS and 2 wt% PS-An-10. The particle diameter, D_{VS}, change of the PA66/sPS blend with the amount of PS-An-10 is very similar to that of the PA66/PS blend (Table 2). This is reasonable since the morphology of the blends is formed in the melt, that is, amorphous state. This implies that we can predict the effect of a compatibilizer on the blends including sPS based on results for the blends with PS. Thus further analyses are focused on the PA66/PS blends.

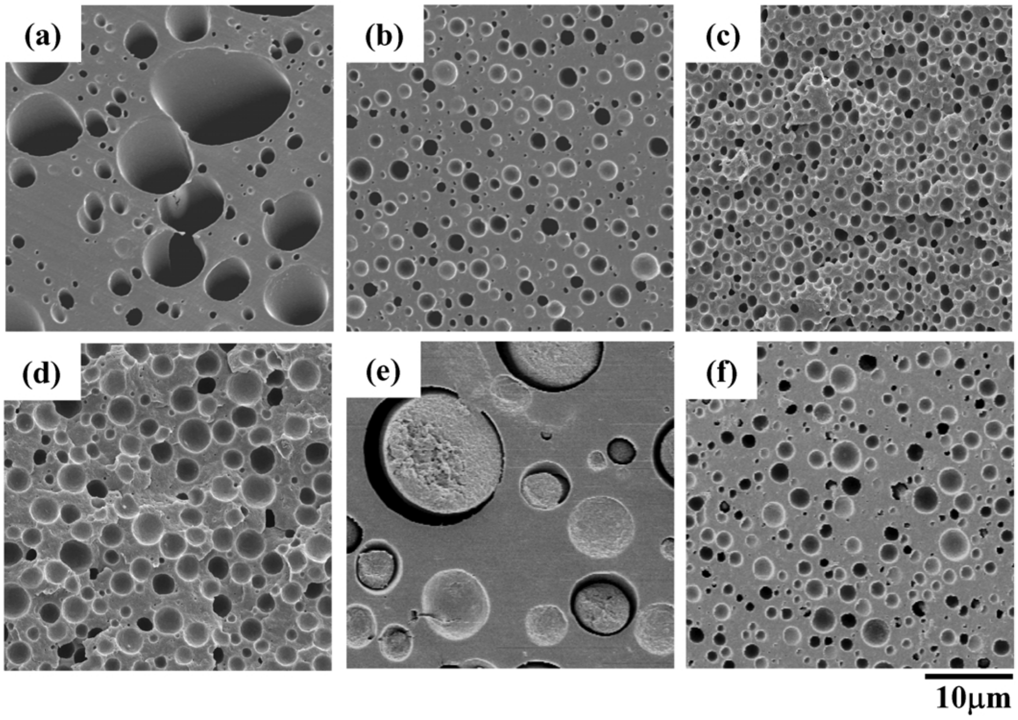

Fig. 4. SEM micrographs of 70/30 PA66/PS blends after 20 min mixing with (a) no functional PS, (b) 2 wt% PS-An-10, (c) 2 wt% PS-An-40, and (d) 1.75 wt% SMA. In (e) and (f), syndiotactic PS replaced PS: (e) no functional PS and (f) 2 wt% PS-An-10.

Table 2
Particle diameter, D_{VS} and interfacial coverage, Σ

Minor phase	Wt% of functional PS[a]	D_{VS}[b] (μm)	Conversion[c] (%)		Σ (chains/nm^2)	Σ/Σ_{max}
			0.5 min	20 min		
PS	0	6.81	–	–	–	–
sPS	0	9.91	–	–	–	–
PS/PS-An-10	2	1.62	82	91	0.80	3.8
	5	0.88	77	92	1.06	5.0
	10	0.63	66	93	1.54	7.3
sPS/PS-An-10	2	1.65	–	–	–	–
	5	1.00	–	–	–	–
	10	0.68	–	–	–	–
PS/PS-An-40	2	1.22	80	92	0.14	0.8
	5	0.77	83	87	0.21	1.2
	10	0.56	80	89	0.31	1.8
PS/SMA	1.75	2.70	64	60	0.55	3.2[d]
	3.5	2.55	63	55	0.95	5.6[d]
	10	1.36	67	37	0.97 (1.76)[e]	5.7[d] (10.4)[d,e]

[a] The amount added to the blend without accounting the functionality.
[b] After 20 min mixing.
[c] Conversion for end-functional PS was normalized by its functionality.
[d] Number of PA66 graft per chain was taken as 2 for Σ_{max}.
[e] Calculated for the conversion at 0.5 min mixing.

D_{VS} vs. wt% of functional PS in the blends is shown in Fig. 5. The weight percent of PS-An in Fig. 5 is the actual amount of phthalic anhydride terminal PS which was obtained by multiplying the amount initially added to the blend by its functionality. At the amounts of functional PS less than 4 wt%, PS-An-40 seems to be slightly more efficient in decreasing D_{VS}. Diameter vs. wt% PS-An are independent of molecular weight above 4 wt%. However, the blends with SMA have larger D_{VS} for all the blend compositions studied.

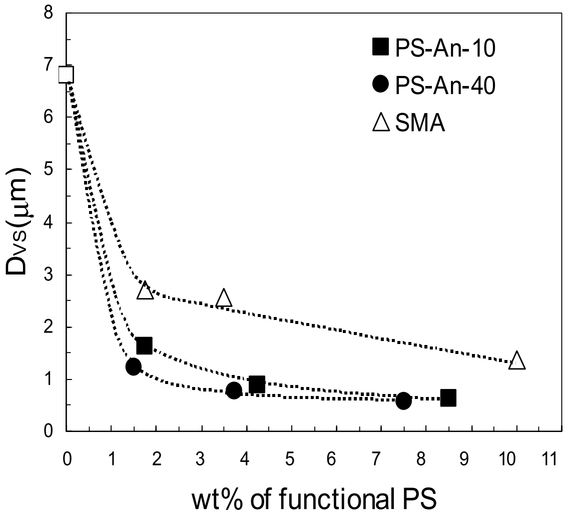

Fig. 5. Volume to surface area average particle size, D_{VS} vs. wt% of anhydride functional PS added to 70/30 PA66/PS blend. Filled squares and circles are for PS-An-10 and PS-An-40 and open triangle is for SMA. Dashed lines are for guiding eyes.

3.2. Reaction conversion

Trifluoroacetylation of PA66 and GPC analysis with the fluorescence detector enabled us to assess the reaction conversion in the blends with mixing time. Even though GPC traces for the block copolymer, PA66-*b*-PS, produced by coupling between PA66 and PS-An were broad (see Fig. 6(a)), we were able to measure conversion within the error of ± 10% by subtracting the peak for the pure PS-An. For instance, Fig. 6(b) shows the trace from the blend with 2 wt% PS-An-10 after 0.5 min mixing and peak I for PA66-*b*-PS-10 after subtracting peak II for the pure PS-An-10. We observed about 1% degradation at 0.5 min which appears as a small bump of peak I at 23.5 ml, and this degradation increased to 5% at 20 min. For reaction conversion, only the area under the main peak of peak I was measured and its ratio to the peak area before subtraction was calculated.

For the blends with SMA, degradation of SMA was observed even after 0.5 min mixing as the tail between 24 and 25 ml in Fig. 6(c), and the peak subtraction used for the blends with PS-An could not be used. Thus, the peak was separated into four peaks at about 17.5 (I), 19 (II), 21 (III) and 23.5 (IV) ml by Gaussian deconvolution as shown in Fig. 6(d) to estimate the conversion to SMA-*g*-PA66. It should be noted that deconvolution into four peaks was decided to obtain peak III with similar polydispersity and elution volume to that of the pure SMA. The peaks I and II at shorter elution volumes were attributed to SMA-*g*-PA66. M_ns of the peaks I and II were estimated to be 208 and 55 kg/mol corresponding to approximately 6 and 1 PA66 grafts per chain, respectively. It should be noted that hydrodynamic volume of graft copolymer was neglected in

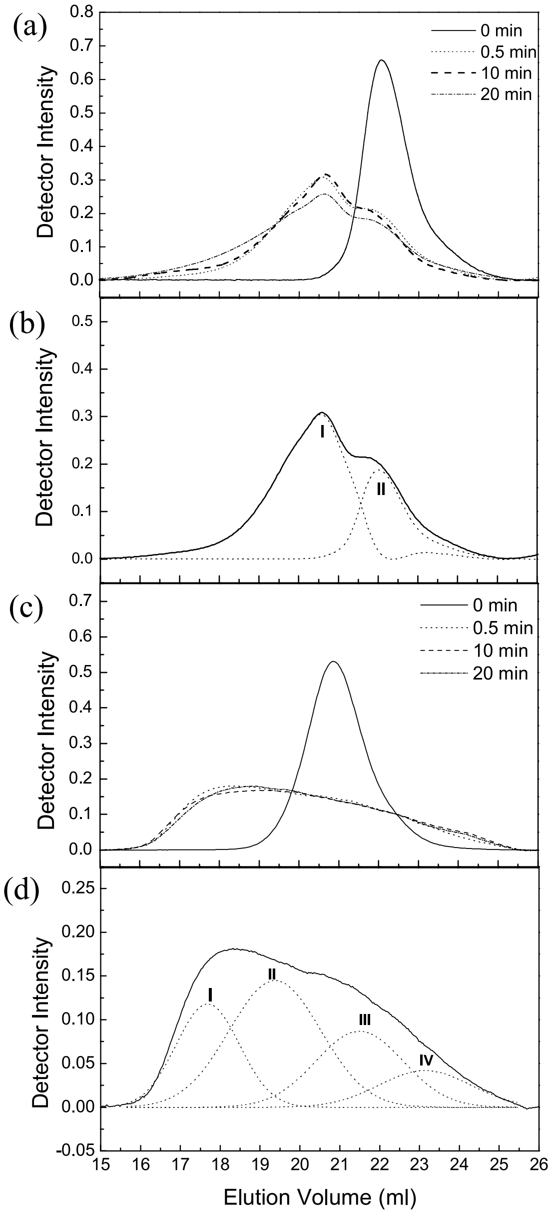

Fig. 6. (a) GPC traces from the 70/30 PA66/PS blend with 2 wt% of PS-An-10 with mixing time; (b) shows the GPC trace at 0.5 min separated into peaks I and II for PA66-b-PS-10 and unreacted PS-An-10, respectively, by peak subtraction. (c) GPC traces from the blend with 1.75 wt% of SMA with mixing time. For the blends with SMA, Gaussian deconvolution was used to estimate reaction conversion as shown in (d) for 0.5 min mixing. Each GPC trace has been normalized to have a peak area of 1. Solid curves in (a) and (c) are for the pure functional PS.

the estimation of the number of grafted PA66 per SMA chain. Also, it should be noted that M_n of PA66 based on PS standards was 33.5 kg/mol. From the sum of the peaks I and II, we were able to approximate M_n of SMA-*g*-PA66 formed in the blend to be 75 kg/mol. Thus, the average number of grafted PA66 per chain was calculated to be 2, which was used for further analyses and discussion. M_n of the peak III was measured to be 13 kg/mol corresponding to the unreacted SMA even though it is slightly lower than the original M_n of SMA, 16 kg/mol. The degradation of SMA was estimated to be about 15% by measuring the area of the peak IV ($M_n = 4.5$ kg/mol) for the blend with 1.75 wt% SMA, and it was almost constant for all the blends containing SMA except for the blend with 10 wt% SMA. This degradation seems to be related to mixing with PA66 since we did not observe this degradation for SMA only under the same condition.

Fig. 7(a) shows a representative example of conversion with mixing time for the blends with PS-An-10 and SMA. Conversion has been normalized with the functionality of PS-An. All the blends with PS-An-10 generated ~90% coupling in 1 min of mixing. This fast reaction and high conversion were also observed for the blends with PS-An-40 (see Table 2).

The amount of PA66-*b*-PS in the blends was calculated using conversion data and the block copolymer molecular weights. Wt% of PA66-*b*-PS-10 vs. mixing time is given in Fig. 7(b). For PA66-*b*-PS, it was assumed that only diblock copolymer was formed even though PA66 might have some diamino end-functional chains which can be the source of triblock copolymer. This was qualitatively confirmed by

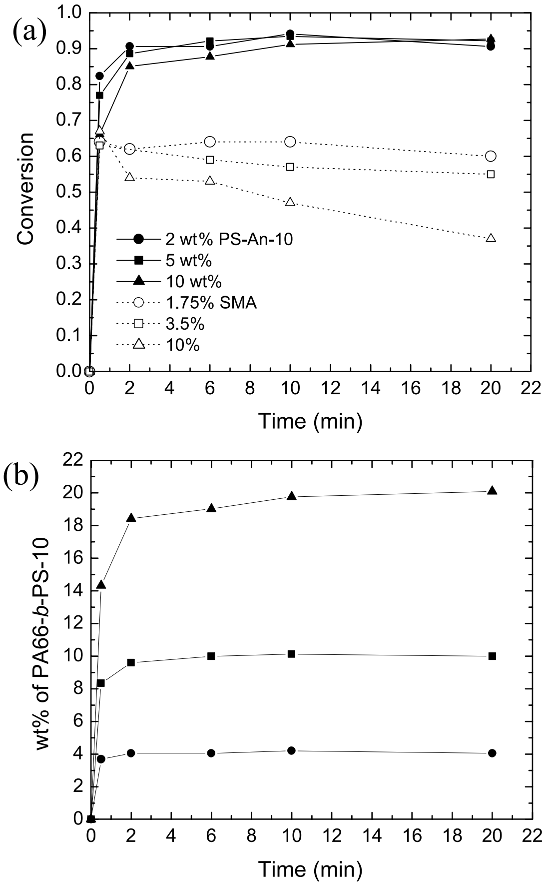

Fig. 7. (a) Conversion to reactively formed copolymer as a function of mixing time in 70/30 PA66/PS with various amounts of functional PS (2 wt%—circle, 5 wt%—square, and 10 wt%—triangle) at 270 °C. Filled and open symbols represent the blends with PS-An-10 and SMA, respectively. Conversion in the blends with PS-An was normalized with its functionality. (b) Amounts of reactively formed block copolymers corresponding to the conversion in (a) for the blends with PS-An-10.

measuring M_n of the peaks for the reactively formed block copolymer which were obtained by the peak subtraction. The M_n of PA66-*b*-PS-10 was determined to be about 45 kg/mol, which is close to the sum of M_n of PA66, 33.5 kg/mol, and that of PS-An-10, 10 kg/mol. For PA66-*b*-PS-40 from PS-An-40, the M_n was 77 kg/mol. The amount of reactively formed block copolymer was in proportion to the amounts of PS-An added to the blends as shown in Fig. 7(b).

In the case of the blends with SMA, ~65% conversion was obtained at 0.5 min and decreased to 60, 55, and 37% at 20 min for the blends with 1.75, 3.5, and 10 wt%, respectively, as shown in Fig. 7(a) and Table 2. The large decrease in reaction conversion with time for the blend with 10 wt% SMA was unexpected. However, this abnormal result can be explained by hydrolysis of PA66 due to water produced by the reaction of amine and anhydride. It has been reported that hydrolysis during PA-anhydride reaction is strongly dependent on the concentration ratio of amine to anhydride [31]. When there was more amine than anhydride, PA chain rupture by hydrolysis giving more amine groups and lowering molecular weight was negligible. If hydrolysis of PA66 occurs during mixing, it is expected that the molecular weight of PA66 in the graft copolymer as well as PA66 in matrix would be lowered resulting in peak shift to larger elution volume in GPC chromatograms. For the 70/30 PA66/PS blends with the concentration ratio of amine to anhydride larger than 1, we did not observe noticeable change of GPC trace with mixing time. Among the blends studied, only the blend with 10 wt% SMA has a higher anhydride concentration, 57.1 μmol/g (PA66) vs. 22.6 μmol/g (PA66) for the amine. Fig. 8 shows the change of the GPC trace with time for the blend. It is clearly seen that the peak shifted to larger elution volume. This implies that the hydrolysis ruptured the PA66 grafts of SMA-*g*-PA66 formed in the blend with 10 wt% SMA. Thus, even though actual conversion at 20 min is similar to or higher than that at 0.5 min, the conversion measured by GPC could be lower since we simply used the Gaussian peak deconvolution.

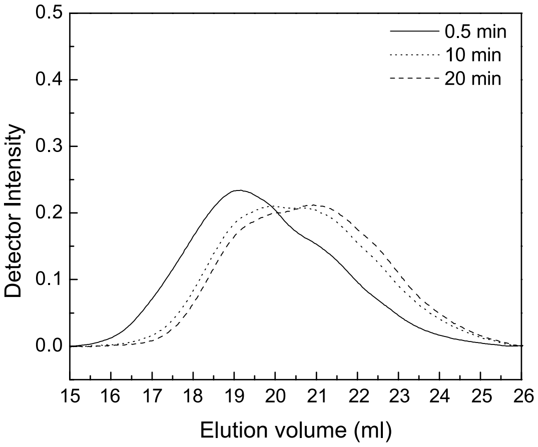

Fig. 8. GPC traces for the blend with 10 wt% SMA with mixing time. As mixing time increased the peak moved to larger elution volume, that is, lower M_n. This was attributed to the hydrolysis of PA66.

4. Discussion

4.1. Reactively formed block copolymers (PA66-b-PS)

Interfacial coverage, Σ, has been used to understand interfacial tension, coalescence of dispersed phase, and interfacial reaction kinetics in immiscible polymer blends compatibilized with copolymers or reactive polymers. Here, we estimated Σ from the amount of reactively formed block copolymers in the blends using Eq. (3) (Table 2).

$$\Sigma = \frac{\phi_f f_{cp} N_{av} \rho_{PS} D_{VS}}{6M_{n,PS}} \tag{3}$$

where ϕ_f is the weight fraction of reactive polymer in the PS phase, f_{cp} the conversion of functional polymer to copolymer measured by GPC, N_{av} the Avogadro's number, ρ_{PS} the density of PS (0.93 g/cm^3 at 270 °C) [32], and $M_{n,PS}$ the number average molecular weight of functional PS. In Table 2, the estimated Σ values are listed.

Maximum coverage, Σ_{max} based on a lamellar spacing of pure diblock copolymer, λ, was also estimated to compare with Σ obtained in the blends (Eq. (4)) [33,34].

$$\Sigma_{max} = \frac{(\lambda/2)}{Na^3} = \frac{N_{av}(\lambda/2)}{M_n/\rho} \tag{4}$$

where the values of λ are 18.5 and 32.5 nm for PA66-*b*-PS's with 10 and 37 kg/mol PS block, respectively [35,36], N is the degree of polymerization of block copolymer, M_n the number average molecular weight of block copolymer, a the statistical segment length of block copolymer. ρ is the density of block copolymer and calculated by $\rho = \phi_{PA66}\rho_{PA66} + (1-\phi_{PA66})\rho_{PS}$ where ϕ_{PA66} is the weight fraction of PA66 in block copolymer, and $\rho_{PA66} = 0.989$ g/cm^3 at 270 °C [36]. Thus, giving the Σ_{max} values of 0.21 and 0.18 chain/nm^2 for PA66-*b*-PS's with 10 and 37 kg/mol PS block, respectively.

Values of Σ/Σ_{max} are shown in Table 2. $\Sigma/\Sigma_{max} > 1$ generally implies that a portion of the reactively formed PA66-*b*-PS exists in bulk phases. For all blends except for the blend with 2 wt% PS-An-40, $\Sigma/\Sigma_{max} > 1$. We examined morphology using TEM as shown in Fig. 9. In Fig. 9(a), no micelle-sized particles were observed in the PA66 matrix of the blend with no functional PS, while the blend with PA66-*b*-PS-10 had tiny particles with diameter ~50 nm as shown in Fig. 9(b). These tiny particles were found even at 0.5 min mixing. On the contrary, micelles (particles with a diameter smaller than 100 nm) were seldom observed in the blend with 2 wt% PS-An-40 showing consistency with the Σ/Σ_{max} result (Fig. 9(c) and Table 2). However, when we increased the amount of PS-An-40 to 5 and 10 wt%, micelles were found, as shown in Fig. 9(d). In order to compare with the

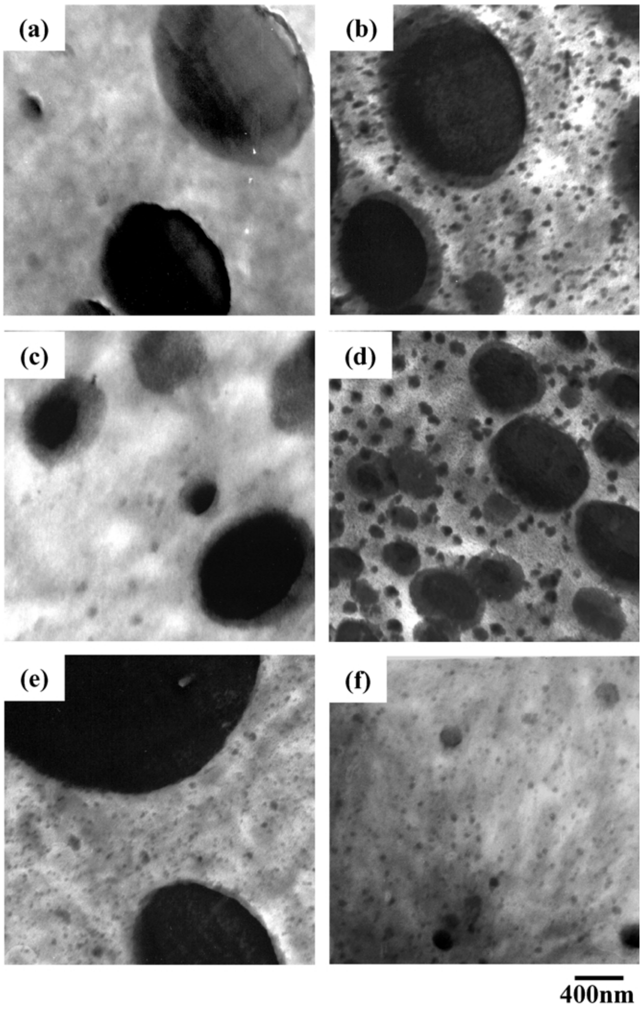

Fig. 9. TEM micrographs of the blends after 20 min mixing with (a) no functional PS, (b) 2 wt% PS-An-10, (c) 2 wt% PS-An-40, (d) 10 wt% PS-An-40, (e) 1.75 wt% SMA. For the comparison, TEM micrograph of the 98.6/1.4 wt/wt PA66/PA66-b-PS-40 is shown in (f).

micelle size of the corresponding block copolymer, PA66-*b*-PS-40, we prepared 98.6/1.4 wt/wt PA66/PA66-*b*-PS-40 blend by melt-mixing 98.7/1.3 wt/wt PA66/PS-An-40 at 270 °C for 20 min. Fig. 9(f) shows the micelles dispersed in PA66, with a size of ~40 nm which is similar to that of the smallest particles observed in Fig. 9(b). This implies that the particles in Fig. 9(b) and (d) are micelles swollen by the PS homopolymer, that is, microemulsions.

Microemulsion formation in reactively compatibilized blends has been explained by interfacial roughening [14–18]. For an interface crowded with block copolymers, the interfacial tension approaches zero, and it becomes rough. This corrugated interface can produce the microemulsions. χN and Σ are known to mainly govern interfacial roughening [18]. It is expected that $\chi N \gg 10$ results in $\Sigma \leq \Sigma_{\max}$, thus no severe roughening [14,16]. For PA66/PS in this study, $\chi = 0.646$ at 270 °C and PS-An was diluted with the nonfunctional PS. Thus, we predicted that interfacial roughening could hardly happen and conversion would be very low. On the contrary, we observed ~80% conversion at 0.5 min mixing even for the blend with 2 wt% PS-An regardless of its molecular weight. This is believed to be due to the extremely fast reaction at this temperature which overcomes the restriction by χN and low concentration of the functional PS. Using activation energy, $E_a = 70$ kJ/mol[37], the amine/anhydride reaction at 270 °C is 28 times as fast as that at 180 °C, which is the common processing temperature for PS/PMMA blend [38].

Now, we suggest the mechanism of microemulsion formation in the PA66/PS blends with PS-An. At the very early mixing time (<0.5 min) the blends would have much less interfacial area than at the later stage of mixing. The high reaction conversion measured at 0.5 min for the blends with PS-An suggests that the interface was saturated with PA66-*b*-PS and rough even earlier than 0.5 min. It is speculated that the mechanical force by external flow would greatly accelerate the microemulsion formation by cutting or pinching off easily the roughened interface at the very early stage of mixing. This is rather different from the role of external flow on micelles formation in a reactive blend claimed by Inoue et al. [19–21]. They have argued that reactively formed copolymer chains could be pulled out from the interface by external flow and form micelles in the bulk phase depending on its molecular architecture, molecular weight, and the applied shear stress. In this case, one should observe the small micelles of pure diblock copolymer unswollen by homopolymer and a narrow micelle size distribution. However, as mentioned above, the micelles in the PA66/PS are swollen by PS homopolymer, giving bigger size and broader size distribution than the micelles of pure diblock copolymer (Fig. 9(b), (d), and (f)). Therefore, we believed that the microemulsions were formed via interfacial roughening caused by the extremely fast reaction and accentuated by external flow.

Increasing the molecular weight of PS-An from 10 to 37 kg/mol delayed microemulsion formation to the larger amounts of PS-An-40 as shown in Fig. 9(c) and (d). Since we observed almost complete conversion in 0.5 min for all the blend compositions, there is no doubt that $\Sigma > \Sigma_{\max}$ at the earlier mixing time. It is believed that increased χN of PA66-*b*-PS-40 affected interfacial roughening. In addition, the interface would be more rigid than that covered with PA66-*b*-PS-10 resulting in less fluctuation. The symmetry of the block copolymer would also influence the curvature of the roughened interface. The interface with asymmetric block copolymer would have a higher curvature toward a phase where a longer block resides. In our case, the radius of gyration, R_g, of the PA66 block is estimated to be 4.8 nm using [36]

$$\frac{\langle r^2\rangle_0^{1/2}}{M_{\mathrm{PA66}}^{1/2}}$$

where $\langle r^2\rangle_0^{1/2}$ is the end-to-end distance. R_gs of the PS blocks in the PA66-*b*-PS's with 10 and 37 kg/mol PS blocks are 1.4

and 5.2 nm, respectively, and have a statistical segment length, $a = 0.67$ nm [39]. This simple analysis indicates that PA66-*b*-PS-40 is more symmetric, while the PA66 block is 3.4 times as bulky as the PS block of PA66-*b*-PS-10. Thus, the interface saturated with PA66-*b*-PS-10 would become corrugated with a higher curvature toward the PA66 matrix than that covered by PA66-*b*-PS-40.

However, the restrictions were overcome by further increasing the amount of PS-An-40 in the blends, and the interfacial regions with sufficient roughness gave rise to the microemulsions. Also, the curvature difference discussed above can influence the amount of PS homopolymer trapped in the microemulsions giving the different sizes (~50 nm vs. ~100 nm) shown in Fig. 9(b) and (d). This molecular weight effect on interfacial roughening leads us to conclude that higher molecular weight and symmetric reactively formed block copolymer is more stable at the interface, and thus plays a better role as a compatibilizer.

4.2. Reactively formed graft copolymer (SMA-*g*-PA66)

Σ and $\Sigma/\Sigma_{\max}$ were also estimated for the reactively formed SMA-*g*-PA66 (see Table 2). To calculate Σ, it is not necessary to know the number of PA66 grafted to a SMA chain. However, the number of grafting chains is necessary to calculate $\Sigma_{\max}$ because of the M_n of the copolymer term in Eq. (4), and it has been estimated to be 2. We neglected maleic anhydride contribution to the parameters such as density and χ used for calculating $\Sigma_{\max}$. For the blend with 10 wt% SMA the values at 0.5 min shown in brackets and at 20 min were estimated since the conversion decreased with mixing time. The values of $\Sigma/\Sigma_{\max}$ in Table 2 are larger than 1 for all blend compositions. Fig. 9(e) shows the smaller micelles dispersed in PA66 with a narrower size distribution than in the blend with PA66-*b*-PS. We attribute this difference between PA66-*b*-PS and SMA-*g*-PA66 to the effect of the molecular architecture of the copolymers. Based on the area ratio of the peak I to the peaks I + II shown in Fig. 6(d), more than 35% of SMA-*g*-PA66 has six PA66 grafts and produces a brush-like structure. It should be noted that the absolute molecular weight of SMA-*g*-PA66 is larger than the measured value by GPC because the hydrodynamic volume of a graft copolymer is smaller than that of linear block copolymer. As a result, the graft copolymer is very asymmetric, and can easily migrate from the interface to the PA66 phase thermodynamically even if interface is not so rough.

In addition, in the calculation of interfacial coverage of SMA-*g*-PA66, we neglected the effect of incorporation of polar maleic anhydride (MA) groups in PS. This would be reasonable if SMA-*g*-PA66 has one or two PA66 grafts. However, because the SMA backbone is more polar than PS, the graft copolymer with more PA66 grafts can escape from the interface and reside in the PA66 matrix more easily. Therefore, the reactively formed SMA-*g*-PA66 studied here is much less stable at the interface than the PA66-*b*-PS-10, and most of them migrated to form micelles in PA66. This instability can be reduced by incorporating a higher molecular weight SMA or reducing the MA functionality.

5. Conclusions

The effect of reactively formed block and graft copolymers on compatibilization of 70/30 wt/wt PA66/PS blends has been investigated by observing morphology and measuring reaction conversion. Anhydride functional polystyrenes were loaded from 0 to 10 wt% in the blends. The reaction conversion with processing time was successfully measured by GPC by employing fluorescent labels, that is, anthracene for phthalic anhydride terminal PS (PS-An) and pyrene for styrene-maleic anhydride copolymer (SMA), and by modifying PA66 via trifluoroacetylation.

We observed extremely fast reaction with the conversion >60% in 0.5 min mixing regardless of the molecular weights and structure and the amount of functional PS's. From the comparison of the PS particle sizes and the estimation of interfacial stability by observing micelles, it was found that the higher molecular weight PS-An-40 is the most effective compatibilizer, showing finer morphology and higher interfacial stability. This implies that symmetric reactively formed block copolymer with higher molecular weight is desirable for reactive compatibilization. Blends of PA66 with syndiotactic PS compatibilized with PS-An gave very similar morphology to the PA66/PS blends indicating that these conclusions apply also to PA66/sPS blends.

Acknowledgements

The research was supported by grants from the Dow Chemical Co. and by the MRSEC Program of the National Science Foundation under Award Number DMR-0212302. The authors thank Thomas R. Hoye in Department of Chemistry for helpful discussions, Jianbing Zhang for providing PS-An-40, and the Dow Chemical Co. for permission to publish this work.

References

[1] Kohan MI, editor. Nylon plastics handbook. New York: Hanser; 1995.
[2] Baker W, Scott C, Hu G-H, editors. Reactive polymer blending. Hanser: Munich; 2001.
[3] Park CD, Jo WH, Lee MS. Polymer 1996;37:3055.
[4] Dedecker K, Groeninckx G. Macromolecules 1999;32:2472.
[5] Chang FC, Hwu YC. Polym Engng Sci 1991;31:1509.
[6] Jo WH, Kim HC. Polym Bull 1992;27:465.
[7] Chiang C-R, Chang F-C. Polymer 1997;38:4807.
[8] Dedecker K, Groeninckx G. J Appl Polym Sci 1999;73:889.
[9] Jones MA, Carriere CI, Dineen MT, Balwinski KM. J Appl Polym Sci 1997;64:673.

[10] Malanga M. Adv Mater 2000;12:1869.

[11] Li H-M, Shen Z-G, Zhu F-M, Lin S-A. Eur Polym J 2002;38:1255.

[12] Zhang XQ, Son Y. J Appl Polym Sci 2003;89:2502.

[13] Hong BK, Jo WH, Kim J. Polymer 1998;39:3753.

[14] Lyu S-P, Cernohous JJ, Bates FS, Macosko CW. Macromolecules 1999;32:106.

[15] Jiao J, Kramer EJ, de Vos S, Moeller M, Koning C. Macromolecules 1999;32:6261.

[16] Yin Z, Koulic C, Pagnoulle C, Jérôme R. Langmuir 2003;19:453.

[17] Yin Z, Koulic C, Pagnoulle C, Jérôme R. Macromolecules 2001;34: 5132.

[18] Jones TD, Schulze JS, Macosko CW, Lodge TP. Macromolecules 2003;36:7212.

[19] Charoensirisomboon P, Chiba T, Solomko SI, Inoue T, Weber M. Polymer 1999;40:6803.

[20] Charoensirisomboon P, Inoue T, Weber M. Polymer 2000;41:4483.

[21] Pan L, Chiba T, Inoue T. Polymer 2001;42:8825.

[22] Jacobi E, Schuttenberg H, Schulz RC. Makromol Chem Rapid Commun 1980;1:397.

[23] Weisskopf K, Meyerhoff G. Polymer 1983;24:72.

[24] Moon B, Hoye TR, Macosko CW. Macromolecules 2001;34:7941.

[25] Moon B, Hoye TR, Macosko CW. Polymer 2002;43:5501.

[26] Yin Z, Koulic C, Pagnoulle C, Jérôme R. Macromol Symp 2003;198: 192.

[27] Matyjaszewski K, Nakagawa Y, Gaynor SG. Macromol Rapid Commun 1997;18:1057.

[28] Park E-S, Kim M-N, Lee I-M, Lee HS, Yoon J-S. J Polym Sci, Part A: Polym Chem 2000;38:2239.

[29] Nemeth S, Jao T-C, Fendler JH. J Photochem Photobiol, A: Chem 1994;78:229.

[30] Maric M, Ashurov N, Macosko CW. Polym Engng Sci 2001;41:631.

[31] Marechal P, Coppens G, Legras R, Dekoinck J-M. J Polym Sci, Part A: Polym Chem 1995;33:757.

[32] Richardson MJ, Savill NG. Polymer 1977;18:3.

[33] Bates FS, Fredrickson GH. Phys Today 1999;52:32.

[34] Macosko CW, Guegan P, Khandpur AK, Nakayama A, Marechal P, Inoue T. Macromolecules 1996;29:5590.

[35] λ for PA66-*b*-PS was calculated by $\lambda \sim 1.03a\chi^{1/6}N^{2/3}$ [33] where a was calculated by the relation in Eq. (4), and χ between PA66 and PS was estimated to be 0.646 by $\chi = (V_{\text{ref}}/RT)(\delta_{\text{PA66}} - \delta_{\text{PS}})^2$ using the solubility parameters of PA66 and PS, $\delta_{\text{PA66}} = 22.87\ \text{MPa}^{0.5}$ and $\delta_{\text{PS}} = 18.6\ \text{MPa}^{0.5}$, respectively, [36] the reference volume, V_{ref}, temperature, T, and the gas constant, R. Here, V_{ref} was estimated by $V_{\text{ref}} = (\nu_{\text{PA66}} M_{0,\text{PA66}} \nu_{\text{PS}} M_{0,\text{PS}})^{0.5}$ where $\nu_{\text{PA66}}(= 1.01\ \text{cm}^3/\text{g})$ and $\nu_{\text{PS}}(= 1.08\ \text{cm}^3/\text{g})$ [32,36] are the specific volumes of PA66 and PS, respectively, at 270 °C, and M_0 is the molecular weight of a monomer.

[36] Brandrup J, Immergut EH, editors. Polymer handbook, 4th ed. ; 1998.

[37] Padwa AR, Sasaki Y, Wolske KA, Macosko CW. J Polym Sci, Part A: Polym Chem 1995;33:2165.

[38] Orr CA, Cernohous JJ, Guegan P, Hirao A, Jeon HK, Macosko CW. Polymer 2001;42:8171.

[39] Russell TP, Menelle A, Hamilton WA, Smith GS, Satija SK, Majkrzak CF. Macromolecules 1991;24:5721.